

This study investigates the process that forms centerline porosity in the axial zone of a continuously cast steel billet during its hardening. The task addressed relates to the need to establish rational parameters for the temperature-speed mode of casting to minimize axial porosity, which is critical for increasing the density of the metal and the quality of rolled products.

A comprehensive methodology for physical modeling of the hardening process using stearin as a model substance has been devised. Based on the analysis of similarity numbers (Biot, Fourier, Kosovych), the exact scales of modeling were established: by time – 1.854, by linear dimensions – 0.1778, by heat transfer coefficient – 0.04639. It was determined that for an adequate simulation of the formation of the bloom blank, the closing angle of the liquid core varies within 2.3–6°. Quantitative parameters of the experiment on the model were established: overheating of the melt in the range of 1.8–4.2°C, which corresponds to 15–35°C for steel.

The resulting data are explained by the laws of convection heat transfer and phase transition. The angle of inclination of the crystallization front and the intensity of heat removal determine the moment of formation of "bridges" and interceptions in the thermal center, which directly defines the morphology and volume of shrinkage pores.

Unlike conventional mathematical modeling, the proposed approach provides high visual reliability of defect formation due to the use of the π -theorem for the selection of physical parameters. This makes it possible to investigate critical system states without the risk of emergencies in industrial settings.

The research results could be used for implementation at metallurgical enterprises in the design and optimization of billet cooling modes on a continuous billet casting machine (CCM), which will ensure an increase in the yield of suitable metal.

Keywords: continuous billet, centerline porosity, physical modeling, similarity numbers, temperature-speed regime, stearin

STUDY OF THE REGULARITIES OF CENTERLINE POROSITY FORMATION IN CONTINUOUSLY CAST BILLETS DEPENDING ON CASTING PARAMETERS

Yevhen Synehin

PhD, Associate Professor*

ORCID: <https://orcid.org/0000-0002-9983-3971>

Volodymyr Ruban

Corresponding author

Doctor of Philosophy (PhD)*

E-mail: v.o.ruban@ust.edu.ua

ORCID: <https://orcid.org/0000-0002-6617-296X>

Kostiantyn Niziaiev

Doctor of Technical Science*

ORCID: <https://orcid.org/0000-0002-9260-0964>

Oleksandr Stoianov

PhD, Associate Professor*

ORCID: <https://orcid.org/0000-0002-7136-7403>

Svitlana Zhuravlova

PhD, Associate Professor*

ORCID: <https://orcid.org/0000-0002-8519-5155>

*Department of Iron and Steel Metallurgy
Ukrainian State University of Science and Technology
Nauky ave., 4, Dnipro, Ukraine, 49005

Received 19.01.2026

Received in revised form 26.03.2026

Accepted 06.04.2026

Published 30.04.2026

How to Cite: Synehin, Y., Ruban, V., Niziaiev, K., Stoianov, O., Zhuravlova, S. (2026). Study of the regularities of centerline porosity formation in continuously cast billets depending on casting parameters. *Eastern-European Journal of Enterprise Technologies*, 2 (1 (140)), 105–114. <https://doi.org/10.15587/1729-4061.2026.356920>

1. Introduction

Centerline porosity is a defect that forms in the central part of ingots and billets during its hardening and is characterized by the concentration of large and small pores along its thermal center. The reasons for the formation of the centerline porosity are the specific conditions of the formation of the continuously cast billets, associated with the formation of a relatively deep core of liquid metal. The crystallization front along the height of the billets due to the considerable length of the liquid metal core converges to the end of solidification at a very small angle, which determines the presence of bridges and interceptions in the center of the billets, which form shrinkage shells.

The nature of the formation and the size of the shrinkage cavities in the axial zone of the billets depend on the amount and speed of metal shrinkage. These processes are determined

by the grade of steel, casting speed, intensity of secondary cooling, cross-sectional dimensions of the billets, and a number of other technological factors. Increased temperature and casting speed contribute to the development of centerline porosity, as the length of the liquid core of the metal increases. The phenomenon of centerline porosity is most developed during high-speed casting of small cross-section billets. It also tends to increase when casting high-carbon grades of steel.

There is a certain dependence between the type of porosity and the crystalline structure of the billets. Concentrated porosity is usually found under a developed columnar structure and is concentrated along the vertical axis in the form of discontinuous cavities. Diffuse porosity develops in the zone of equiaxed crystals and the limited zone of columnar dendrites. With such a structure of a continuously cast billet, shrinkage porosity is formed in the form of numerous small pores.

Reducing the level of centerline porosity is an urgent task for improving the quality of steel products. One of the effective approaches to the study of this phenomenon is to investigate conditions for the formation of the centerline porosity in a continuous billet, which allows one to gain a deeper understanding of the mechanisms behind porosity formation and to optimize the technological parameters of the process.

2. Literature review and problem statement

Internal blank defects, particularly centerline porosity and shrinkage, caused by poor feeding of the axial zone at the end of solidification, reduce the density of the central zone of the billet and the quality of the final products. An additional factor that worsens the effect of shrinkage processes on the quality of ingots and blanks is the content of sulfur in the metal. Effective metal desulfurization is an important factor in reducing the probability of the formation of centerline porosity of a continuously cast billet [1]. The method of injecting dispersed magnesium through a submerged rotating nozzle enables deep cleaning of the metal from sulfur, which contributes to improving its purity, reducing the number of non-metallic inclusions and more uniform crystallization. This, in turn, has a positive effect on the macrostructure of the workpiece, minimizing chemical heterogeneity and gas saturation, which ultimately reduces the formation of defects. Also, to overcome these defects, such methods of external dynamic impact on the metal as dynamic soft pressing, electromagnetic stirring, vibration treatment, etc. are used [2–12].

The authors of paper [2] conducted an analysis of the thermomechanical connection, in particular, the formation of central shrinkage porosity and the influence of casting parameters were investigated. Thermomechanical analysis using the finite element method made it possible to investigate the process of formation of central shrinkage porosity, which is inaccessible to conventional methods. Increased pouring speed from 1.6 to 2.8 m/min reduces the displacement of the center of the workpiece and reduces the tendency to porosity. Increasing superheat of liquid steel from 10 to 40°C also reduces the displacement of the center of the workpiece, although the effect is less pronounced. These factors confirm the possibility of slightly controlling the formation of porosity through the optimization of technological parameters. However, the authors of the work did not establish quantitative regularities of the influence of overheating and the speed of spillage on the dimensions of the centerline porosity. This is related to the complex mechanism of centerline porosity formation, which includes thermophysical, hydrodynamic, and thermodynamic processes.

In [3], the influence of the range and amount of dynamic soft crimping (DSR) was investigated using a verified heat transfer model and physical properties of GCr15 steel. The optimal DSR parameters were determined based on the simulation results for two options that differ in the pouring speed and the fraction of the solid phase during crimping. The second crimping option (pour speed 0.75 m/min and solid phase fraction 0.3–1.0) showed significantly less segregation and a more uniform distribution of carbides compared to the first option (pour speed 0.85 m/min and solid phase fraction 0.6–1.0). It was confirmed that the central segregation is inherited from the bloom to the bar, despite partial improvement during heating and rolling. To improve the internal quality, it is necessary to minimize the carbon content in the later stages of solidification, choose the optimal location of DSR (solid phase

fraction 0.3–1.0) and apply intensive crimping. At the same time, the cited work does not provide an explanation regarding the influence of the location of DSR and the carbon content in the remains of the liquid phase in the axial zone of the continuously cast workpiece.

Optimum crimping zone is critical to reduce segregation, as premature crimping increases the risk of cracking and late crimping is ineffective. The size of the liquid core of the workpiece and the distance between the branches of the secondary dendrites are also important factors. The authors of [4] investigated a new scheme, including sequential multi-roll soft pressing and single-roll strong pressing, and successfully obtained a high-carbon steel billet with high uniformity produced by a continuous casting process. However, the lack of reliable methods for determining the position of the crystallization front and the length of the liquid core of the workpiece makes it difficult to study the regularities of the influence of soft crimping on the formation of centerline porosity.

The authors of paper [5] claim that the soft crimping method (TSR) leads to an improvement in the internal quality of the continuously cast billet, however, its use can cause internal and surface cracks. Optimizing the TSR parameters for 82A steel reduced centerline porosity, V-segregation and central segregation of the billet while controlling cracking. Modeling of heat exchange taking into account thermophysical parameters showed that the optimal location of TSR is at a distance of 6.96–8.46 m from the meniscus at a cooling intensity of 2.2 m³/h. The study also found that a combination of electromagnetic stirring (F-EMS) and TSR achieves the best stock quality, with F-EMS more effectively reducing center segregation and TSR reducing V-segregation and porosity. This once again confirms the need to build deterministic mathematical models to describe the influence of pouring parameters on the formation of centerline porosity.

In [6], a method of pretreatment by crimping is proposed to reduce the centerline porosity in large blanks. It was established experimentally and by the method of modeling that the use of a temperature gradient helps increase the deformation of the center, and effective closing of the pores is achieved at a deformation of 0.16–0.22. When exceeding 0.25, the porosity is concentrated in the center, increasing the risk of defects. Analysis of hydrostatic integration confirmed its suitability for evaluating the degree of pore closure, which emphasizes the prospect of the method for improving the quality of continuously cast blanks.

In work [7], the principles of the formation of the main internal defects that arose in the blanks with different compression zones after the subsequent rolling process were investigated, from the point of view of local distribution and formation of the microstructure. The correct selection of the crimping zone and its intensity helps improve the density and chemical homogeneity of the metal. In particular, the use of active crimping rollers can significantly reduce the level of porosity in the central zone of the workpiece, ensuring uniform compaction of the metal. However, under the conditions of incorrect setting of the mechanical crimping mode, additional internal defects may be formed, in particular, microcracks and uneven microstructure. Thus, the cited studies once again confirm that the effectiveness of mechanical crimping largely depends on the accuracy of process control, which should be based not on optimization carried out under the conditions of a specific enterprise, but on deterministic mathematical models that are universal for different pouring conditions and grade assortment of steel.

Experimental studies of the vibration effect on the surface of a workpiece 150×150 mm in size with a 20–30% liquid core content in the central part were conducted by the authors of work [8]. Macro- and microstructural analysis revealed that vibration reduces the centerline porosity and shrinkage shells, and small dendrites grow in the intergranular voids of the central zone of the workpiece due to the improvement of the flowability of the metal in the two-phase zone. In addition, compositional analysis revealed a more uniform distribution of carbon in the center of the workpiece after vibration exposure, and the density of the central region of such workpieces was higher, while the low density zones were significantly reduced. At the same time, the difficulty of introducing vibrational oscillations to the workpiece during the pouring process slows down the study of quantitative patterns of the influence of vibration on the quality of the workpiece.

Electromagnetic stirring (EMS) has become a common practice in continuous casting to reduce defects, particularly centerline porosity and dendritic segregation. EMS systems are characterized by high energy consumption and reduced reliability, which is explained by their external placement and the need to use complex cooling mechanisms [9].

Paper [10] is aimed at studying the effect of combined electromagnetic stirring on the reduction of centerline porosity during horizontal continuous casting of billets made of SUS347 steel containing Nb. For continuous pouring of a round workpiece with a diameter of 263 mm, combined electromagnetic stirring was used in the crystallizer (M-EMS), in the ZVO (S-EMS) and in the zone of final crystallization (F-EMS). Three-stage mixing proved to be the most effective, while the absence of one of the methods reduces the effect. S-EMS promotes the enlargement and dispersion of equiaxed grains and prevents them from falling out in the later stages of solidification. The optimal zone for the application of F-EMS is a liquid core diameter of 40–80 mm. F-EMS by itself has little effect on the structure of the workpiece but enables maintaining the liquid mobility of the solid-liquid phase with a high content of the solid phase.

The authors of [11] proposed an approach to improve the quality of the continuously cast billet, based on the pulsed supply of inert gas to the metal in the crystallizer of the continuous casting machine (CCM) and stepwise soft crimping of the billet in the secondary cooling zone of CCM. The impact of pulsed inert gas supply on the formation of the hardening model and the dependence of the width of the columnar-crystalline zone on the inert gas consumption and the frequency of pulsations have been established. Also, on the basis of the authors' physical modeling of crimping of a continuously cast workpiece using shear in the secondary cooling zone of a continuous casting machine (CCM), a mechanism for eliminating centerline porosity was established, which shows that the use of shear improves the elimination of defects. At the same time, it is difficult to assess the individual impact of each of the influences on the formation of the centerline porosity.

Technical solutions for improving the crystallization process due to pulsating blowing of metal with inert gas in the crystallizer and shear clamping of the workpiece in the secondary cooling zone of the continuous casting machine are given in work [12]. The physical simulation of shear compression of continuously cast blanks in the secondary cooling zone of CCM on model ingots showed a positive effect on the reduction of the zone of columnar crystals and reduction of the centerline porosity.

Our review of the literature [1–12] shows that current research is mostly focused on the use of energy-intensive methods of external influence, such as electromagnetic stirring, mechanical compression, or vibration processing. At the same time, the issue of establishing the boundary conditions for the formation of the centerline porosity purely through the control of the parameters of the temperature-speed mode of pouring remains insufficiently elucidated. In particular, the lack of visualization of mechanisms behind the closing of the crystallization front and the formation of "bridges" in the liquid well under conditions of variable heat flow complicates the development of rational cooling modes without the use of complex technical systems.

The above allows us to state that it is appropriate to conduct a study aimed at establishing quantitative regularities in the influence of hardening parameters on the morphology of the axial zone of a continuously cast workpiece using physical modeling methods.

3. The aim and objectives of the study

The purpose of our study is to establish quantitative regularities in the influence of the temperature-speed parameters of pouring and the closing angle of the liquid hole on the mechanism behind the formation of the centerline porosity of the continuously cast billet by means of physical modeling based on the similarity theory. This will make it possible to design and implement rational cooling regimes at metallurgical enterprises, which could ensure the minimization of axial defects and the increase of metal density without the use of additional energy-intensive methods of external influence.

To achieve the goal, the following tasks must be solved:

- to justify parameters for the physical modeling of the hardening process of a steel billet based on the theory of similarity;
- to determine parameters for the physical model, perform the factorization of the system, and form the experiment plan;
- to analyze the combined effect of overheating parameters and cooling intensity on the morphology of the axial zone to determine the critical conditions for the transition from a porous to a dense structure of the workpiece.

4. The study materials and methods

The object of our research is the process that generates centerline porosity in the axial zone of a continuously cast steel billet during its hardening.

The principal hypothesis assumes that the minimization of axial porosity could be achieved without the use of energy-intensive methods of external influence purely by establishing a rational combination of melt overheating and heat transfer intensity, which ensure the optimal closing angle of the liquid well, which prevents the premature formation of "bridges" in the thermal center.

In the work, a number of assumptions are adopted, in particular, the change in the thickness of the solid crust over time is described by the law of the square root. The thermophysical properties of the model substance (stearin) are considered stable within the investigated temperatures. To simplify the study, the hardening process is considered to be a two-dimensional problem in the cross section of the workpiece. The effect of the ferrostatic pressure of the melt and the release of dissolved gases on the formation of the pore volume is not

taken into account. The cooling intensity along the height of the coolers of the model is assumed to be uniform, which simulates the averaged heat transfer coefficient in the cooling zones of CCM.

We propose investigating the process of feeding the axial zone of a continuously cast workpiece with liquid metal using stearin as a model substance. The closing angle of the crystallization front at the final stages of solidification of the continuously cast billet can be simulated by changing the angle of inclination to the vertical surface of the coolers of the model, on which stearin is solidified.

Therefore, this study was carried out using physical modeling as in industrial settings it would require rather large costs. The plan of an active experiment may contradict the technological instructions and lead to the formation of defects and emergencies [13]. We note significant losses of finished products for making longitudinal templates of blanks, which are necessary for further analysis. Mathematical modeling is also impractical, as the obtained results may have significant deviations due to the presence of a large number of uncontrolled factors [14]. Computer simulation requires expensive licensed software, which is also not devoid of the drawbacks of mathematical modeling. From this point of view, physical modeling is an expedient solution.

The experimental setup is shown in Fig. 1. Stearin of grade (DSTU 7620:2014) with a solidification temperature range of 54–60°C was used as a material imitating steel [15]. The required amount of stearin was weighed on electronic scales to ensure the same length of all test samples. To prevent significant overheating, stearin was melted in a water bath. Before pouring the molten stearin, according to the experiment planning matrix, copper coolers 6 were installed at a given angle, which varied within 2.3–6° to the vertical. All units of the installation were hermetically fixed to avoid leaks of stearin. Experiments were photographed on a camera installed before installation.

The experimental setup consists of two hollow copper coolers 6, rectangular cross-section with internal space dimensions of 26 × 31 mm. Together with two glass plates 7 and rubber bottom 8, they form the working space of the installation. Sensors of electronic thermometers 5 are attached to the inner surface of one of the coolers and to the outer surface of the glass, which measure the surface temperature of the copper cooler and the glass, respectively. Other sensors for measuring the temperature of cooling air are installed in silicone tubes at the inlet and outlet of copper coolers 6.

Molten stearin was poured into the installation through a preheated stearin temperature funnel between glass plates. Overheating of stearin before pouring was chosen according to the planning matrix of our experiment in the range of 1.8–4°C. Since the liquidus temperature of stearin significantly depends on its chemical composition, its value, which was 55.6°C, was previously determined by constructing a thermo-kinetic diagram. The temperature of the molten stearin was measured with an electronic thermometer with an accuracy of 0.1°C. In the case of excessive overheating, it was cooled by adding small portions of

stearin shavings, while stirring with a large piece of stearin or a metal rod.

In accordance with the selected similarity numbers and the calculated simulation scales, the air that is blown into the system by compressor 1 was chosen as the cooler. To improve the cooling efficiency of the sample, the air before entering coolers 6 passes through cooler 2. To collect excess moisture from the air behind cooler 2, condenser 3 is installed. The volumetric air flow rate is measured with the float rotameter 4 RM-2.5 GUZ (Ukraine).

Starting from the moment of pouring, every 5 min we recorded the readings of all thermometers and air consumption for cooling. Due to the rapid change in the indicators of the devices after filling, during the first 5 minutes, the indicators were recorded every 2 minutes. The moment of complete solidification of the sample was determined visually. The air temperature in the room was measured with an electronic thermometer XH-W1209 (China). Each measurement was accompanied by photography on a digital camera in HD quality (1280 × 720 pixels).

After complete cooling, the obtained sample was cut along a vertical plane parallel to the wider faces and scanned on a Lexmark X1130 Series multifunction device scanner (USA) with a resolution of 1200 dpi.

The following methods were used to solve our tasks. To justify the choice of model substance, calculation of scale coefficients (by time, geometry, and heat transfer) and ensuring the adequacy of the physical model to real processes, the method of dimensional analysis and similarity theory (π -theorem) was used in CCM. To visualize the hardening process and study the mechanisms of the formation of axial porosity with the help of transparent crystallizers and stearin, the method of physical modeling was applied. The method of visual control was used to study the transverse templates of the model blank in order to assess the shape and size of the resulting porosity. The analysis of the results from a series of experiments and the establishment of mathematical relationships between the closing angle of the hole and the shape of the shrinkage cavity were carried out by the statistical data regression analysis method.

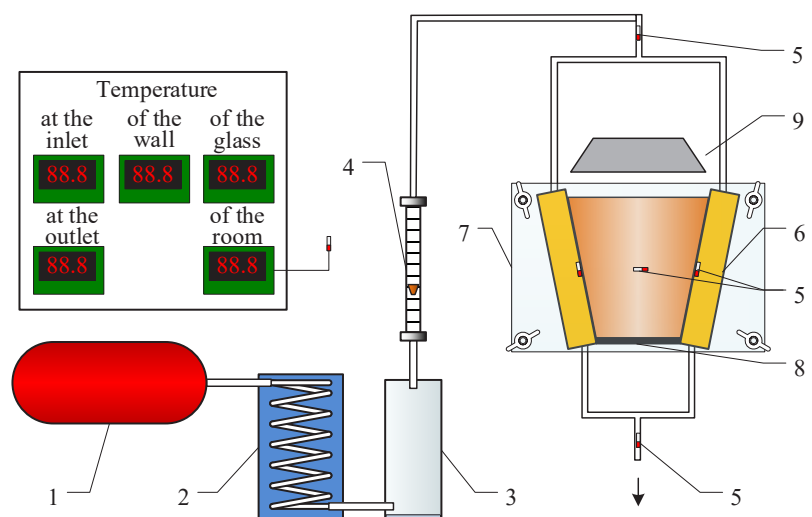


Fig. 1. Schematic of the experimental installation:

- 1 – a compressor with a capacity of 1.5 kW and a capacity of 200 l/min; 2 – air cooler; 3 – condenser for collecting moisture; 4 – float rotameter type RM-2.5 GUZ; 5 – sensors of electronic thermometers; 6 – copper coolers; 7 – glass plates; 8 – rubber bottom; 9 – a lampshade with a 12 W lamp for heating the upper part of the sample

5. Results of studies on the formation of the centerline porosity of a continuously cast billet

5.1. Determining similarity numbers for physical modeling

The key task in finding similarity numbers for physical modeling is the selection of the most significant parameters that affect the process under study. Taking into account all parameters of the process in the model makes its simulation impossible since it will be impossible to choose model substances and conditions of the experiment similar to the real analog.

According to [16, 17], an important role in the formation of the centerline porosity is also played by the closing angle of the liquid hole at the final stages of solidification of the workpiece. The similarity of this angle on the model can be ensured by giving the cooling surface a certain taper, the value of which can be calculated based on the pouring modes. The tangent of angle φ of the inclination of the crystallization front to the workpiece axis is equal to the ratio of thickness ξ of the solid crust formed along the h length of the workpiece section (Fig. 2).

Assuming that the thickness of the crust changes over time according to the law of the square root, a formula for determining angle φ depending on the pouring mode is derived

$$\operatorname{tg} \varphi \equiv \frac{\xi}{h} = \frac{k\sqrt{\tau}}{h} = \frac{k\sqrt{\frac{h}{w}}}{h} = \frac{k}{\sqrt{hw}}, \quad (1)$$

where k is the hardening coefficient of the workpiece, $\text{m}/\text{min}^{0.5}$; h – length of the studied section of the workpiece (Fig. 1), m ; w – speed of drawing the workpiece, m/min .

For the pouring conditions of the bloom billet calculated from formula (1), the value of angle φ ranges within $2.3\text{--}6^\circ$, depending on the pouring speed of the cooling conditions and the grade of steel being poured.

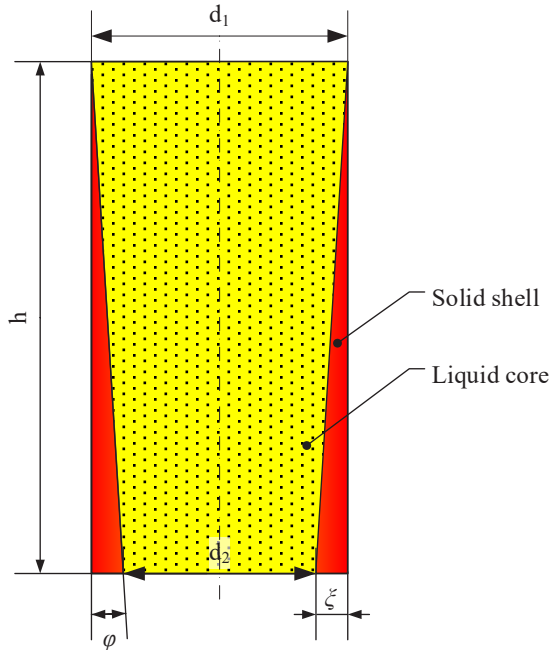


Fig. 2. Ensuring the similarity of the closing angle of the liquid hole

The main requirement when conducting physical modeling is to observe the most complete similarity of the processes

on the sample model. According to the theorem of similarity, it is possible to ensure similarity only if the determining numbers of similarity are equal on the sample and the model. Therefore, determining the type of similarity numbers is one of the most important modeling tasks.

At the first stage, based on the analysis of the process and logical considerations, a set of independent physical quantities that characterize the physical system of the sample being modeled is compiled. To implement this process, a set of parameters was chosen, including the temperature difference between the liquid and the solid surface Δt , the hardening time τ , and the coefficient of heat transfer from the cooling surface of the crystallizer to the refrigerant α . The cross-section of workpiece l , the density of liquid ρ , the specific heat capacity of liquid c_p , the coefficient of thermal conductivity of solid phase λ , the specific heat of solidification Q_0 , the overheating of the liquid above liquidus temperature Δt_z are taken into account. The formation of dimensionless similarity numbers according to the π -theorem is given in Table 1 [11].

Table 1

Reducing the studied parameters to dimensionless similarity numbers

| No. | Parameter | Unit of measurement | Order of magnitude | Primary factors | Similarity number |
|-----|--------------|------------------------------------------------------------------|--------------------|------------------|----------------------------------------------------------------------|
| 1 | Δt | $^\circ\text{C}$ | 10^2 | $^\circ\text{C}$ | – |
| 2 | τ | s | 10^3 | s | – |
| 3 | α | $\frac{\text{kg}}{(\text{C} \cdot \text{s}^3)}$ | 10^2 | – | $\pi_1 = \frac{\alpha \cdot \Delta t \cdot \tau^3}{\rho \cdot l^3}$ |
| 4 | l | m | 10^{-1} | m | – |
| 5 | ρ | $\frac{\text{kg}}{\text{m}^3}$ | 10^3 | kg | – |
| 6 | C_p | $\frac{\text{m}^2}{(\text{C} \cdot \text{s}^2)}$ | 10^2 | – | $\pi_2 = \frac{C_p \cdot \Delta t \cdot \tau^2}{l^2}$ |
| 7 | λ | $\frac{\text{kg} \cdot \text{m}^2}{(\text{C} \cdot \text{s}^3)}$ | 10^1 | – | $\pi_3 = \frac{\lambda \cdot \Delta t \cdot \tau^3}{l^4 \cdot \rho}$ |
| 8 | $Q_0(t, L)$ | m^2/s^2 | 10^2 | – | $\pi_4 = \frac{Q_0 \cdot \tau^2}{l^2}$ |
| 9 | Δt_z | $^\circ\text{C}$ | 10^1 | – | $\pi_5 = \frac{\Delta t_z}{\Delta t}$ |

Similarity numbers were reduced to generally accepted ones that describe processes by means of modification. Using the transformation of complexes π_1 and π_2 , we obtained a dimensionless complex in the form of the Biot number (Bi), which is a measure of the ratio of internal and external thermal resistances

$$\frac{\pi_1}{\pi_3} = \frac{\alpha \cdot \Delta t_z \cdot \tau^3}{\rho \cdot l^3} \cdot \frac{\lambda \cdot \Delta t_z \cdot \tau^3}{l^4} = \frac{\alpha \cdot l}{\lambda}. \quad (2)$$

Using the transformation of complexes π_4 and π_2 , we obtained a dimensionless complex in the form of the phase transition number (Kosovich number) K , which shows the ratio of the heat of the phase transition (crystallization) to the heat of heating or cooling

$$\frac{\pi_4}{\pi_2} = \frac{Q_0 \cdot \tau^2}{l^2} \cdot \frac{C_p \cdot \Delta t_z \cdot \tau^2}{l^2} = \frac{Q_0}{C_p \cdot \Delta t_z}. \quad (3)$$

Using the transformation of complexes π_3 and π_2 , we obtained a dimensionless complex in the form of the Fourier number Fo, which shows dimensionless time. It characterizes the relationship between the rate of change of the temperature field, physical properties, and body dimensions

$$\frac{\pi_3}{\pi_2} = \frac{\lambda \cdot \Delta t_z \cdot \tau^3}{l^4 \cdot \rho} \cdot \frac{C_p \cdot \Delta t_z \cdot \tau^2}{l^2} = \frac{\lambda \cdot \tau}{l^2 \cdot \rho \cdot C_p} = \frac{\alpha \tau}{l^2} \tag{4}$$

This complex was used to determine the scale of hardening time on the model and prototype.

5. 2. Justification of modeling parameters and experiment planning

According to the results of our calculations and based on the reference literature [18], the modeling parameters for the experimental set-up were calculated: heat transfer coefficient, overheating of the paraffin before pouring, etc.; their values are summarized in Table 2.

Taking into account the significant duration of the experiment and the material costs for its implementation, a fractional-factorial experiment (FFE) with three factors and variation of each at three levels FFE 3^{3-1} was chosen for physical modeling.

The model that describes the process is stepwise; therefore, to find the regression coefficients, we reduce it to a linear form by logarithmization. To determine the regression coefficients, logarithms of Biot, Kosovich (phase transition number), and $\text{lg}tg\varphi$ numbers should be used.

The value of the similarity numbers at the zero level is calculated from the following formula [19]

$$\Pi_i^0 = 10^{\frac{\text{lg} \Pi_i^{\text{max}} + \text{lg} \Pi_i^{\text{min}}}{2}}$$

For the calculated three levels of factors, the values of air flow, overheating above the melting temperature (55.6°C), and angle φ were calculated. The standardization of factor scales is given in Table 3.

According to the obtained values, the FFE planning matrix was built and the levels of variation in model parameters were established (Table 4).

The established parameters of the experimental plan allowed us to proceed to the implementation of a series of model experiments. The data obtained on the basis of this standardization will be used to evaluate the adequacy of the model and analyze the conditions for the formation of the centerline porosity.

Table 2

Range of variation in the selected parameters on the model and in reality

| No. | Parameter | Value | | Scale |
|-----|-------------------------------------------------------------------------------------|-----------------|----------|---------|
| | | For model | Actual | |
| 1 | Temperature difference between liquid and solid surface Δt | 11.8286–43.2106 | 98–358 | 0.1207 |
| 2 | Hardening time τ | 6257.25 | 3375 | 1.854 |
| 3 | Heat transfer coefficient α | 23.195–46.39 | 500–1000 | 0.04639 |
| 4 | The width of the workpiece l | 0.08 | 0.45 | 0.1778 |
| 5 | Density of substance ρ [18] | 812 | 7800 | 0.1041 |
| 6 | Specific heat capacity of substance C_p [18] | 3.22 | 0.69 | 4.6667 |
| 7 | Thermal conductivity coefficient λ [18] | 0.24 | 29.1 | 0.0082 |
| 8 | Specific heat of solidification Q_0 [18] | 150.1 | 267.5 | 0.5611 |
| 9 | Overheating of steel Δt_{st} | 1.8–4.2 | 15–35 | 0.1207 |
| 10 | The angle of inclination of the crystallization front in the crystallizer φ | 2.3–6 | 2.3–6 | 1 |

Table 3

Standardization of factor scales

| Plan characteristics | $x_1 = \text{lg}Bi$ | $x_2 = \text{lg}K$ | $x_3 = \text{lg}tg\varphi$ |
|----------------------|-----------------------------|---------------------------|------------------------------|
| Zero level | 1.0436 | 1.2285 | -1.1873 |
| Variation range | 0.1489 | 1.2923 | 0.2089 |
| Upper level | $\text{lg}15.6146 = 1.1935$ | $\text{lg}25.85 = 1.4125$ | $\text{lg}0.1051 = -0.9784$ |
| Lower level | $\text{lg}7.83 = 0.8938$ | $\text{lg}11.08 = 1.0445$ | $\text{lg}0.04016 = -1.3962$ |

Table 4

The FFE planning matrix and the levels of variation in model parameters

| Experiment No. | Order | $x_0 - \text{lg}A$ | $x_1 - \text{lg}Bi$ | $x_2 - \text{lg}K$ | $x_3 - \text{lg}tg\varphi$ |
|------------------------------|-------|--------------------|---------------------|--------------------|----------------------------|
| 1 | 8 | 1 | -1 | -1 | 1 |
| 2 | 2 | 1 | -1 | 0 | 0 |
| 3 | 9 | 1 | -1 | 1 | -1 |
| 4 | 5 | 1 | 0 | -1 | 0 |
| 5 | 1 | 1 | 0 | 0 | 0 |
| 6 | 7 | 1 | 0 | 1 | 0 |
| 7 | 4 | 1 | 1 | -1 | -1 |
| 8 | 6 | 1 | 1 | 0 | 0 |
| 9 | 3 | 1 | 1 | 1 | 1 |
| Parameter value on the model | | | Air consumption, % | Overheating, °C | φ |
| Maximum level | | | 30 | 4.2 | 6 |
| Zero level | | | 21.4 | 2.8 | 3.7 |
| Minimum level | | | 0 | 1.8 | 2.3 |

5. 3. Analysis of critical conditions for the formation of "bridges" and interceptions in the thermal center of the workpiece

Scanned images with a resolution of 2400 dpi were obtained from the sample sections. The resulting frames allow us to evaluate the behavior of the formation of the structure of the workpiece, in particular, the critical factors of the formation of the centerline porosity, which affect the quality of the continuously cast workpiece. Fig. 3 shows cross-sections of samples of the first, second, and third experiments, which illustrate a clearly defined shrinkage shell formed in the upper part, indicating the zone of completion of solidification of the steel billet.

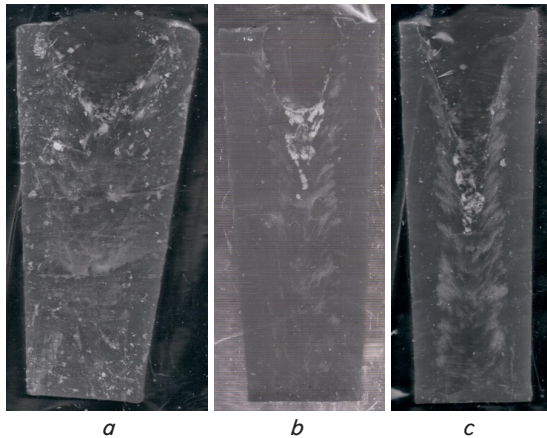


Fig. 3. Samples of the angle of convergence γ in the shrink shell (scale 1:1): *a* – experiment 1; *b* – experiment 2; *c* – experiment 3

Fig. 4, 5 show sections of sample blanks from the fourth to sixth, and from the seventh to ninth experiments, respectively. The images contain macro sections of the cross-section of samples of continuously cast model blanks, which demonstrate the formation of the shrinkage shell.

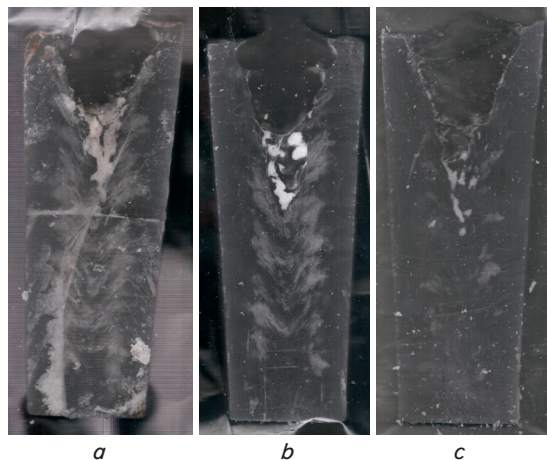


Fig. 4. Samples of the angle of convergence γ in the shrink shell (scale 1:1): *a* – experiment 4; *b* – experiment 5; *c* – experiment 6

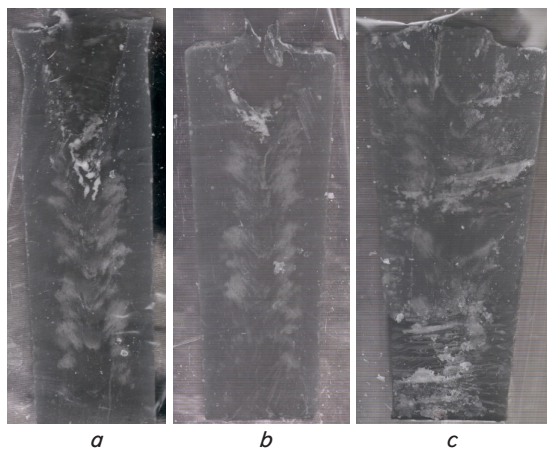


Fig. 5. Samples of the angle of convergence γ in the shrink shell (scale 1:1): *a* – experiment 7; *b* – experiment 8; *c* – experiment 9

To assess the propensity of the workpiece model to the formation of centerline porosity, the angle of convergence γ in the shrinkage shell of the workpiece model was chosen [20]. In the case of using the depth of the shrinkage shell as an objective function, it is impractical since the shrinkage voids in the continuously cast billet are discontinuous and are usually estimated at the factory by their diameter.

On the basis of our research, from the obtained images of the blanks, the angle of convergence γ in the shrink shell was measured by using Microsoft Excel (USA). The results were entered into a spreadsheet for regression analysis. The estimation of the coefficients of the regression equation was calculated using the method of least squares. The statistical indicators of the resulting mathematical model are given in Table 5

$$\gamma = Bt^{0.56} \cdot K^{-0.37} \cdot \text{tg}^{0.94}\varphi. \tag{5}$$

Table 5

Statistical indicators in the resulting mathematical model

| Parameter | $\gamma = b_0 \cdot Bt^{b_1} \cdot K^{b_2} \cdot \text{tg}^{b_3}\varphi$ | | | |
|------------------------------------------------------------------------|--------------------------------------------------------------------------|-------|--------|-------|
| | b_0 | b_1 | b_2 | b_3 |
| Regression coefficients | 1.016 | 0.561 | -0.370 | 0.936 |
| Standard error | 0.124 | 0.138 | 0.147 | 0.180 |
| Student's <i>t</i> -test | 8.228 | 4.053 | 2.515 | 5.193 |
| Critical value of the Student's <i>t</i> -test $t_{cr}(\alpha = 0.05)$ | 2.422 | | | |
| Multiplier <i>R</i> | 0.953 | | | |
| Approximation coefficient R^2 | 0.909 | | | |

The resulting mathematical relationship quantitatively describes the relationship between the cooling conditions and the morphology of the shrink shell. This forms a scientific basis for choosing such pouring modes that enable minimization of centerline porosity without involving additional means of impact on the metal.

6. Discussion of results based on investigating conditions for the formation of the centerline porosity in a continuously cast billet

In contrast to studies in which most attention is paid to external methods of influence ("soft" compression [3–7], EMF [5, 9, 10], vibration [8], etc.), our research focuses on the internal resources of the system. The formula (1) that we proposed makes it possible to simulate the process of advancing the crystallization front under the conditions of continuous drawing of the workpiece in CCM using a stationary model. At the same time, it is assumed that the intensity of secondary cooling and, accordingly, the speed of advance of the crystallization front in the zone of secondary cooling is a constant value.

The proposed numbers of similarity ensure the similarity of only heat transfer processes that take place at the final stages of solidification of the workpiece. Observance of complete similarity taking into account capillary phenomena and fluid hydrodynamics in a porous medium is an extremely difficult or completely impossible task, as it requires additional consideration of the surface tension and viscosity of the liquid phase enriched with doping impurities.

Using a fractional factorial experiment design instead of a full factorial experiment has several disadvantages. The most important one is confounding or mixing effects. In the

fractional plan, the assessment of the main factor can be mathematically inextricably linked with the effects of interaction of other factors. In FFE 3^{3-1} plan (9 experiments instead of 27), linear and quadratic effects of one factor can be mixed with paired or triple interactions of others. However, in our case, only linear effects were taken into account, according to which logarithmization and transition to a power model with dimensionless similarity numbers were carried out.

Another disadvantage is that because of the fewer degrees of freedom to estimate the reproduction error, statistical tests such as Fisher's F-test become less sensitive. This increases the risk of second-order error: the conclusion that the factor does not affect the process is false due to insufficient data.

There is also a risk of model bias when the real response surface has complex topography (e.g., a sharp peak or narrow ridge) and the full factorial experiment replica selected for the fractional plan may miss this region entirely. However, the chosen type of step model (step) eliminates this risk.

The empirical mathematical model derived from the results of physical modeling for describing the angle of convergence of the crystallization front can be used to describe the process of formation of the centerline porosity of a continuously cast billet. By changing the opening angle of coolers, we adjusted the initial angle between the crystallization fronts from opposite sides, simulating the angle formed during the movement of the workpiece through the crystallizer (Fig. 2). The filling of the model during physical modeling was carried out quickly enough to avoid a significant difference in the thickness of the crust, which is formed during the filling of the model.

The use of air as a coolant and a certain interval of its consumption makes it possible to ensure compliance of the intensity of cooling with the physical and chemical properties of the model substance (stearin). Stearin, chosen as a model substance, does not form a crystalline structure, but this is not essential for the study of the process of formation of a shrinking shell on a macroscopic scale. Similarly to the prototype, both shrinkage voids and shrinkage looseness were observed on the model of the workpiece, which testifies to the feasibility of using stearin as a model substance.

The angle γ at which the crystallization front connects was chosen as a quantitative indicator characterizing the evolution of centerline porosity. The low value of this angle under certain cooling conditions (Fig. 3, experiment 3) indicates a high probability of the formation of bridges, which complicate the supply of liquid metal to shrink cavities, contributing to their formation. A high value of the angle (Fig. 3, experiment 1), on the contrary, indicates a low probability of the formation of bridges and improvement of the feeding conditions of the axial part of the workpiece at the final stage of its hardening [20].

The constructed empirical model (5) indicates a positive effect on the feeding conditions of the axial part of the workpiece by increasing the cooling intensity (heat transfer coefficient from the surface of the workpiece crust), reducing melt overheating, and reducing the pouring speed. The effect of these casting parameters on the closing angle of the crystallization front of a continuously cast billet is fully consistent with the theoretical provisions of billet structure formation and the practice of steel casting at CCM [20].

Unlike mathematical modeling and analysis by the finite element method [2], in which results often have significant deviations due to the impossibility of taking into account all uncontrolled factors, our result provides high visual reliability of the defect formation process. This becomes possible thanks to the application of physical modeling using the π -theorem

for accurate selection of physical parameters and scales (in terms of time, dimensions, and heat transfer).

The reliability of the results is explained by the fundamental laws of convection heat transfer and phase transition, which are the basis for calculating similarity numbers (Biot, Fourier, Kosovich). Argument that our goal is achieved is based on geometric similarity, thermophysical adequacy, and practical verification.

For an objective evaluation of the results and their implementation in the steelmaking industry, several limitations must be taken into account. The physical model is limited in height, so it does not fully take into account the effect of the ferrostatic pressure of the melt, which in actual industrial installations contributes to the "self-healing" of pores in the lower horizons of the workpiece. In the model, the intensity of heat transfer is averaged through the heat transfer coefficient in the crystallizer and the secondary cooling zone. Under real conditions, the unevenness of irrigation by nozzles and the condition of the surface of the rollers could induce local thermal stresses that the model does not simulate.

A promising area of research is the transition from static parameters to dynamic control over the cooling process in real time using artificial intelligence systems. This could make it possible to automatically adjust the temperature-speed regime depending on the current fluctuations in the chemical composition of the steel and the condition of CCM equipment for guaranteed minimization of axial porosity.

7. Conclusions

1. Based on the similarity theory, the main similarity numbers (Biot, Kosovich, and Fourier numbers) characterizing the thermophysical processes of solidification have been determined. That has made it possible to establish the ranges of variation in the technological parameters on the model (air consumption, overheating, the angle of the crystallization front connection), which correspond to the actual conditions of pouring bloom blanks in CCM.

2. The nature of influence of the main technological factors on the formation of axial defects has been experimentally determined: an increase in the overheating of the melt leads to the expansion of the zone of centerline porosity, while the intensification of heat transfer contributes to its narrowing. It was determined that the closing angle of the liquid hole is a critical factor, increasing the value of which contributes to reducing the risk of defect formation and enables the minimization of discontinuous cavities in the axial zone.

3. Based on the results of our fractional-factorial experiment, an empirical mathematical model $\gamma = Bi^{0.56} \cdot K^{-0.37} \cdot \text{tg}^{0.94} \varphi$, was derived, which describes the dependence of convergence angle in the shrink shell γ on the cooling intensity and temperature-speed parameters. A high coefficient of approximation ($R^2 = 0.909$) confirms the adequacy of our model and the possibility of using it to predict the quality of the axial zone of the workpiece. It was established that an increase in the Biot number (cooling intensity) and the tangent of angle of inclination of the crystallization front (φ) has a positive effect on the growth of angle γ , which improves the conditions of liquid metal feeding of the axial part of the workpiece at the final stage of solidification. On the contrary, an increase in the overheating of the metal (represented by the Kosovich number) leads to a decrease in the angle of convergence, increasing the probability of the formation of "bridges" and shrinkage pores.

Conflicts of interest

The authors declare that they have no conflicts of interest in relation to the current study, including financial, personal, authorship, or any other, that could affect the study and the results reported in this paper.

Funding

The study was conducted without financial support.

Data availability

All data are available in the main text of the manuscript.

Use of artificial intelligence

The authors confirm that they did not use artificial intelligence technologies when creating the current work.

Authors' contributions

Yevhen Synehin: Conceptualization, Methodology, Software, Validation, Formal analysis, Investigation, Writing – original draft, Visualization; **Volodymyr Ruban:** Software, Validation, Formal analysis, Investigation, Writing – review & editing, Visualization; **Kostiantyn Niziaiev:** Investigation, Resources, Project administration, Funding acquisition; **Oleksandr Stoianov:** Methodology, Investigation, Resources, Writing – review & editing; **Svitlana Zhuravlova:** Data Curation, Project administration, Funding acquisition.

References

1. Sigarev, E. N., Chernyatevich, A. G., Chubin, K. I., Zarandiya, S. A. (2011). Desulfurization of hot metal by the injection of disperse magnesium through a submerged rotating tuyere. *Steel in Translation*, 41 (6), 487–491. <https://doi.org/10.3103/s0967091211060155>
2. Wang, X., Guo, Y., Xiao, P., Liu, Z., Zhu, L. (2023). Numerical simulation of shrinkage porosity defect in billet continuous casting. *High Temperature Materials and Processes*, 42 (1). <https://doi.org/10.1515/htmp-2022-0246>
3. Yao, C., Wang, M., Cheng, M., Xing, L., Wang, Y., Gao, Y., Bao, Y. (2022). Effect of Dynamic Soft Reduction Range and Amount on Central Segregation in Bloom and the Resulting Microstructure in the Rod of GCr15-Bearing Steel. *Steel Research International*, 93 (11). <https://doi.org/10.1002/srin.202200495>
4. Gao, Y., Bao, Y., Wang, Y., Wang, M., Zhang, M. (2023). Development of a Novel Strand Reduction Technology for the Continuous Casting of Homogeneous High-Carbon Steel Billet. *Steel Research International*, 94 (5). <https://doi.org/10.1002/srin.202200740>
5. Han, Y., Yan, W., Zhang, J., Chen, W., Chen, J., Liu, Q. (2020). Optimization of Thermal Soft Reduction on Continuous-Casting Billet. *ISIJ International*, 60 (1), 106–113. <https://doi.org/10.2355/isijinternational.isijint-2019-409>
6. Liu, Y., Liu, J., He, Y. (2022). Evolution Behavior and Closure Mechanism of Porosity in Large Billet during the Reduction Pretreatment. *Metals*, 12 (4), 599. <https://doi.org/10.3390/met12040599>
7. Gao, Y., Bao, Y., Wang, M., Zhang, H., Wang, Y. (2024). Investigation on the effect of reduction process on internal quality of high carbon steel billet and its evolution in as-rolled wire rod. *Metallurgical Research & Technology*, 121 (5), 506. <https://doi.org/10.1051/metal/2024058>
8. Shen, C., Liping, W., Qiang, L., Biao, S., Zheng, Y., Chunlin, H. (2019). Research on improving central defects of billet by external vibration strike. *Ironmaking & Steelmaking*, 47 (9), 986–990. <https://doi.org/10.1080/03019233.2019.1652446>
9. Shakhov, S. I., Sivak, B. A., Vdovin, K. N., Shakhov, D. S., Kerimov, R. I., Bairamov, A. T. (2020). Perfection of the equipment of electromagnetic stirring in moulds of billet and bloom CCM. *Ferrous Metallurgy. Bulletin of Scientific, Technical and Economic Information*, 76 (10), 1014–1020. <https://doi.org/10.32339/0135-5910-2020-10-1014-1020>
10. Yamanaka, A., Ota, K., Terunuma, M., Tsujita, S., Abe, T. (1998). Reduction of Center Porosity of Round Billet by Electromagnetic Stirring in Horizontal Continuous Casting. *Tetsu-to-Hagane*, 84 (9), 609–616. https://doi.org/10.2355/tetsutohagane1955.84.9_609
11. Kanaev, A. T., Bykov, P. O., Bogomolov, A. V., Reshotkina, E. N. (2012). Reducing the central porosity of continuous-cast billet by modification of the solidification process. *Steel in Translation*, 42 (8), 643–645. <https://doi.org/10.3103/s0967091212080037>
12. Salina, V. A. (2022). Modeling of a continuously cast billet central porosity reducing processes. *Science and Technology of Kazakhstan*, 4, 59–67. <https://doi.org/10.48081/qfdl7381>
13. Ruban, V., Stoianov, O., Niziaiev, K., Synehin, Y. (2021). Determining changes in the temperature field of a graphitized hollow electrode during metal processing periods in ladle-furnace. *Eastern-European Journal of Enterprise Technologies*, 2 (1 (110)), 109–115. <https://doi.org/10.15587/1729-4061.2021.230002>
14. Myrav'yova, I. G., Ivancha, N. G., Shcherbachov, V. R., Vishnyakov, V. I., Ermolina, E. P. (2023). Improvement of the Burden Column Structure by Controlling the Multicomponent Burden Loading Mode into the Blast Furnace. *Problems of the Regional Energetics*, 2 (58), 138–149. <https://doi.org/10.52254/1857-0070.2023.2-58-12>
15. DSTU 7620:2014. Palm Kernel Stearin. Technical specifications supplement. Kyiv. Available at: https://online.budstandart.com/ua/catalog/doc-page.html?id_doc=92687
16. Mamuzić, I., Longauerova, M., Strkalj, A. (2005). The analysis of defects on continuous cast billets. *Metalurgija*, 44 (3), 201–207. Available at: <https://bucketvirtualpro-private.s3.amazonaws.com/files-bv/20050728/49395.pdf>

17. Yu, H., Zhu, M. (2009). Effect of electromagnetic stirring in mold on the macroscopic quality of high carbon steel billet. *Acta Metallurgica Sinica (English Letters)*, 22 (6), 461–467. [https://doi.org/10.1016/s1006-7191\(08\)60124-6](https://doi.org/10.1016/s1006-7191(08)60124-6)
18. Hress, O. V., Ohurtsov, A. P., Nedopokin, F. V. (2010). *Doslidzhennia, modeliuвання ta optymizatsiya lyvarnykh system*. Dniprodzerzhynsk: DDTU, 282. Available at: https://nmetau.edu.ua/file/gress_o_v__ogurtsov_a_p__nedopokin_f_v_doslidzhennya__modelyuvannya.pdf
19. Lantukh, O. S., Molchanov, L. S., Synehin, Ye. V. (2018). *Metodyka fizychnoho modeliuвання splyvannya ansamblu nemetalevykh vkluchen u stalerozlyvnomu kovshi*. *Matematychno modeliuвання*, 1 (38), 95–99. Available at: https://nmetau.edu.ua/file/kmetsteel_16495.pdf
20. Smirnov, O. M., Kuberskyi, S. V., Shtepan, Ye. V. (2011). *Bezperervne rozlyvannya stali*. Alchevsk: DonDTU, 518. Available at: https://drive.google.com/file/d/1fqRdAAfnynPV47ZFsc9m9y9_9JU8S9eS/view